Volume 16, Number 2, 2023. pp. 215-227

Jordan Journal of Physics

ARTICLE

In-situ Radiometric Assessment of UNESCO World Heritage Sites in Kathmandu Valley of Nepal Using Gamma Ray Spectrometry

Anita Mishra and **Raju Khanal**

Central Department of Physics, Tribhuvan University, Kirtipur, Kathmandu 44613 Nepal.

Doi: **https://doi.org/10.47011/16.2.9**

Received on: 15/09/2021; *Accepted on: 24/10/2021*

Abstract: The paper presents the results of rapid in-situ radiometric assessment of the seven UNESCO Cultural World Heritage Sites of the Kathmandu Valley in Nepal. The geological condition of the valley and NORM present in the building materials of Heritage Sites can increase gamma exposure and, therefore, be hazardous to the public and the environment. The objective of the study is to provide baseline data of annual effective dose (AED) and to assess associated health risks in the surrounding area of World Heritage Sites. The average absorbed dose rates in air and mass concentrations of radioelement ^{40}K, ^{238}U, and ^{232}Th are measured in the range 120.907±11.121 to 152.320±15.072 nGy/h, 2.785±0.734 to 3.458±0.802%, 6.599±2.965 to 8.778±3.379 ppm and 17.744±+5.897 to 25.137±6.959 ppm, respectively. The dose rates contributed by the particular gamma radionuclides are also calculated. The statistical analysis shows that the distribution of dose rates is asymmetric with positive skewness. The dose rates have a high and positive correlation with the mass concentrations of radioelements. From the average measured absorbed dose rate, the AED and excess lifetime cancer risk (ELCR) are estimated. Despite the dose rate being higher than the global average value, it does not pose any radiological health risks to visitors or the public living in the vicinity (<1 mSv/y).

Keywords: Mass concentration, AED, Building material, In-situ measurement, Gamma radiation, UNESCO sites.

Introduction

The exposure to background radiation is caused mainly by natural radiation sources. Thus, the terrestrial gamma radiation is the main source of external exposure radiation [1]. In turn, the natural radionuclides ^{40}K, ^{238}U, and ^{232}Th (primordial radionuclides) found in the upper layer of the Earth's crust constitute the major source of outdoor terrestrial radiation [2]. The level of radioactivity from the primordial radionuclides depends on the geological conditions and the types of rocks and soils [3] [4]. All building materials are derived from rocks and soils containing natural radionuclides (^{40}K, ^{238}U, and ^{232}Th), hence are naturally radioactive [5]. Building materials with above-normal levels of natural radioactivity can also increase radiation exposure [6]. The level of radiation from rocks and soil varies from place to place and the actual level of radiation in a given location can be determined by measuring the external gamma dose rate [1]. The radiological map showing the air-absorbed dose rate gives the estimation of the terrestrial radiation dose to people and can identify the area with natural radiation hazards [7]. In-situ gamma-ray studies are conducted to facilitate rapid and comprehensive mapping, exploration of uranium deposits, and environmental research [2]. The in-situ measurement data were reported in studies conducted in India [8], China [9], Japan [10], Malaysia [11], Kenya [12], etc.

Corresponding Author: Anita Mishra **Email**: anita.745711@cdp.tu.edu.np

The ionizing radiation can damage human cells, causing cancer and hereditary diseases [1]. The aim of this study is to measure the outdoor external gamma dose rates in air and the mass concentrations of radioelement ^{40}K, ^{238}U, and ^{232}Th present in building materials and the Earth's surface to estimate the Annual Effective Dose (AED) received by the people visiting the sites and living nearby. The associated health risk is determined by calculating Excess Lifetime Cancer Risk (ELCR). The values reported in the present study are compared with the values found in other countries and the world average value. The resulting data is a preliminary baseline scientific data of outdoor external gamma radiation dose rate and associated health risks from exposure to the public near and inside the complex of UNESCO World Heritage Sites. So far, there were no reports of measurement of outdoor terrestrial gamma radiation in the complex of UNESCO World Heritage Sites in the Kathmandu Valley.

Materials and Methods

Study Area

There ten UNESCO World Heritage Sites in Nepal, with eight cultural and two natural Heritage Sites. Seven out of eight Cultural Heritage Sites are situated in the Kathmandu Valley. The Kathmandu Valley consists of three cities (Kathmandu, Lalitpur, and Kirtipur) and lies at high altitudes (1235.60 to 1498.09 meters ASL) surrounded by mountains that are up to 3000 meters high. The Kathmandu Valley is densely populated with 20,288 people per square kilometer (worldpopulationreview.com/ worldcities/ kathmandu-population/). The seven UNESCO Cultural World Heritage Sites in the Kathmandu Valley are Bhaktapur Durbar Square, Boudhanath, Changu Narayan, Kathmandu Durbar Square, Pashupatinath, Patan Durbar Square, and Swayambhunath. The four sites (Boudhanath, Changu Narayan, Pashupatinath, and Swayambhunath) are the ancient Hindu and Buddhist temples, while the remaining three (Bhaktapur Durbar Square, Kathmandu Durbar Square, and Patan Durbar Square) are the historical royal palaces. While the World Tourism Organization aims to protect Cultural Heritage Sites and preserve them for future generations (https://www.e-unwto.org/doi/ epdf/10.18111/9789284416608) there is a growing health concern, because the ancient structures are built from materials containing NORM (stones, bricks, clay, cement, concrete, wood, and metals) that can increase the exposure to background radiation. The natural features of the sites include ponds, a river, and thick vegetation. Numerous visitors and pilgrims visit the sites regularly. Also, there are many street shopkeepers and a large population of local residents in the area surrounding these sites. Taken together, all the aforementioned factors warrant the importance of outdoor terrestrial radiation exposure measurements.

The absorbed dose rates in the air from outdoor terrestrial gamma radiation in the complex of seven UNESCO Cultural World Heritage Sites in the Kathmandu Valley were measured. The latitude and longitude from the GPS location along with the altitude of each site are given in Table 1.

TABLE. 1. Latitude, longitude, and altitude of UNESCO sites.

S.N.	Sites	North Latitude (deg)	East Longitude (deg)	Altitude (m)
1	Bhaktapur Durbar Square	27.671736 to 7.672752	85.427025 to 5.429405	1287.31 to 1296.75
2	Boudhanath	27.720417 to 27.722011	85.361313 to 85.362587	1273.76 to 1283.36
3	Changu Narayan	27.716143 to 27.716507	85.427513 to 85.430977	1251.10 to 1498.09
4	Kathmandu Durbar Square	27.699232 to 27.705732	85.301552 to 85.307632	1242.56 to 1254.96
5	Pashupatinath	27.707226 to 27.711079	85.346199 to 85.350250	1252.45 to 1278.21
6	Patan Durbar Square	27.672644 to 27.673796	85.324646 to 85.325561	1250.50 to 1266.12
7	Swayambhunath	27.714342 to 27.718237	85.283722 to 85.293251	1235.60 to 1358.60

In-situ Measurement

The in-situ radiological survey was performed inside and around the UNESCO Cultural Heritage Sites in the Kathmandu Valley with the help of PGIS-2, a portable gamma-ray spectrometer fitted with a 0.34 liter NaI(Tl) crystal. The energy range of the detector is 20 keV to 3 MeV. The detector was carried in a

backpack along the road inside the complex of Heritage Sites with a speed of < 2 km/hr. The Global Positioning System (GPS) location and spectral data were recorded per second in the data logger unit (Android mobile) connected via Bluetooth with the detector. These data were extracted from data logger unit to the personal computer in laboratory and was analyzed using software provided with the detector.

Gamma Ray Spectrometry

The absorbed dose rates in outdoor air in the environment and mass concentrations of radioelement ^{40}K, ^{238}U, and ^{232}Th in building materials and earth surface were measured with the help of a portable gamma-ray spectrometer. The differential portable gamma-ray spectrometer used can record 512 channels of data in the energy range of 0-3 MeV. It was auto-calibrated and had real-time spectrum stabilization by the natural gamma photo peaks. The dose rate and mass concentration of ^{40}K were directly measured from the emission line at 1461 keV while the dose rate and mass concentration of the uranium and thorium decay series were measured from the gamma emission of ^{214}Bi at 1764 keV and ^{208}Tl at 2614 keV, respectively.

Dose Rates from Mass Concentration of Gamma Radionuclides

The theoretical dose rates of 13.078 nGy/h, 5.675 nGy/h, and 2.494 nGy/h per unit radioelement concentration of ^{40}K (%), ^{238}U (ppm) and ^{232}Th (ppm) were used to calculate the dose rate from mass concentrations of gamma radionuclides [2]. Absorbed dose rates in the air from the mass concentration of gamma radionuclides were first calculated separately for ^{40}K, ^{238}U, and ^{232}Th and then summed to get the total dose rate.

Estimation of Outdoor Annual Effective Dose (AED)

The AED is calculated by using a conversion factor of 0.7 Sv/Gy (to convert the absorbed dose rate in the air to the human effective dose equivalent) and an outdoor occupancy factor of 20% [1].

$$\text{AED (nSv)} = \text{D nGy/h} \times 8760 \text{ h} \times 0.2 \times 0.7 \text{ Sv/Gy} \quad (1)$$

where D is the average absorbed dose rate and 8760 is hours in one year.

Estimation of Excess Lifetime Cancer Risk

The ELCR was calculated from Eq. (1) using Eq. (2) [13]:

$$\text{ELCR} = \text{AED} \times \text{LE} \times \text{RF} \quad (2)$$

where LE is life expectancy in Nepal, 66.2 years, (http://en.worldstate.info/Asia/Nepal) and RF is the fatal risk per Sievert, which is 0.055 as recommended by ICRP for the stochastic effect from low dose rate [14]. The average absorbed dose rate was used for the calculation of the annual effective dose.

Radiological Mapping and Contour Map

The PEI Core Software installed in the data logger unit provides the GPS information for each location corresponding to the recorded data. The PEI View software provided with the detector was used to produce KMZ files in Google Earth Pro. The map was prepared using Surfer software and the statistical analysis was done using Grapher software.

Results and Discussion

The measured outdoor absorbed dose rates in air and mass concentrations of radioelement ^{40}K, ^{238}U, and ^{232}Th in the designated sites are given in Table 2. The maximum and minimum dose rates were found in Changu Narayan complex, while the mean dose rate was found minimum in Swayambhunath at 120.907±11.121 nGy/h and maximum in Boudhanath at 152.320±15.072 nGy/h. The mean mass concentration of ^{40}K was found lower in Changu Narayan at 2.785±0.734% and higher in Bhaktapur Durbar Square at 3.458±0.802%. The lower mean mass concentrations of ^{238}U and ^{232}Th were found in Pashupatinath at 6.599±2.965 ppm and Changu Narayan at 17.744±5.897 ppm, respectively, whereas the higher mean mass concentrations of ^{238}U and ^{232}Th at 8.778±3.379 ppm and 25.137±6.959, respectively, were recorded in Boudhanath. The absorbed dose rate contributed from gamma radionuclides ^{232}Th was found higher in all sites compared to that of ^{40}K and ^{238}U, which can be attributed to the presence of crystalline rocks with gneisses, granites, and high and low-grade metasediments in the area. The lower contribution of dose rates from ^{40}K was found in Boudhanath, Changu Narayan, and Swayambhunath, while in Bhaktapur Durbar Square, Kathmandu Durbar Square, and Patan Durbar Square the ^{238}U dose rate was lower. The dose rates from ^{40}K and ^{238}U were found nearly

equal in Pashupatinath (Table 3). The dose rates contributed from the gamma radionuclides ^{40}K, ^{238}U, and ^{232}Th were found higher than the world average value listed in Table 3 [1]. The calculated dose rate from the mass concentrations of gamma radionuclides and the measured dose rate in the air were found nearly equal (Fig. 1). The ratio of the calculated dose rate and the measured dose rate showed no discrepancy in the survey data. The radiological map showing the spatial distribution of dose rates in the survey sites overlaid on a topological map showing altitude contour and imagery map is shown in Fig. 2 and Fig. 3, respectively. The color code is used for absorbed dose rates in air.

TABLE 2. Measured dose rates and mass concentrations of gamma radionuclides ^{40}K, ^{238}U, and ^{232}Th.

	Dose rate (nGy/h)		Conc. of ^{40}K (%)		Conc. of ^{238}U (ppm)		Conc. of ^{232}Th (ppm)	
Sites	Range	Mean	Range	Mean	Range	Mean	Range	Mean
Bhaktapur Durbar Square	109.484 to 206.115	144.023± 15.816	1.382 to 6.535	3.458 ± 0.802	0.636 to 19.269	7.186 ± 3.157	5.437 to 52.637	23.455 ± 6.758
Boudhanath	116.189 to 202.476	152.320 ± 15.072	0.758 to 5.496	3.065± 0.779	1.000 to 22.215	8.778± 3.379	8.505 to 47.555	25.137± 6.959
Changu Narayan	74.987 to 210.148	137.946± 20.735	0.457 to 5.436	2.785± 0.734	1.026 to 22.81	7.320± 3.410	2.128 to 63.786	24.171± 8.156
Kathmandu Durbar Square	93.978 to 190.167	136.013± 18.419	1.087 to 6.648	3.247± 0.835	0.629 to 21.073	7.215± 3.185	2.075 to 55.992	20.101± 6.649
Pashupatinath	89.31 to 176.14	124.876± 19.067	0.274 to 6.399	2.867± 0.920	0.314 to 18.821	6.599± 2.965	1.909 to 48.049	18.607± 6.825
Patan Durbar Square	102.925 to 180.246	138.004± 11.277	1.450 to 6.601	3.403± 0.828	0.626 to 18.316	6.917± 3.036	5.434 to 47.134	21.118± 5.814
Swyambhunath	86.467 to 162.671	120.907± 11.121	0.956 to 5.883	2.832± 0.692	0.528 to 20.316	6.705± 2.879	1.992 to 43.592	17.744± 5.897
World average [32]		58		1.316		2.672		11.083

TABLE 3. Dose rates from gamma radionuclides ^{40}K, ^{238}U, and ^{232}Th calculated from their mass concentrations.

Sites	Dose rate (nGy/h)							
	^{40}K		^{238}U		^{232}Th		Total	
	Range	Mean	Range	Mean	Range	Mean	Range	Mean
Bhaktapur Durbar Square	18.073 to 85.464	45.228 ± 10.493	3.609 to 109.351	40.786 ± 17.916	13.559 to 131.276	58.497 ± 16.852	87.845 to 252.495	144.512 ± 23.358
Boudhanath	9.913 to 71.876	40.091 ± 10.187	5.675 to 126.070	49.818 ± 19.173	21.211 to 118.602	62.691 ± 17.348	88.286 to 234.903	152.601 ± 23.218
Changu Narayan	5.977 to 71.096	36.436 ± 9.610	5.822 to 129.446	41.544 ± 19.355	5.307 to 159.082	60.284 ± 20.343	44.237 to 265.958	138.265 ± 30.595
Kathmandu Durbar Square	14.215 to 86.942	42.470 ± 10.920	3.569 to 119.589	40.947 ± 18.075	5.175 to 139.644	50.133 ± 16.583	60.428 to 234.007	133.550 ± 27.452
Pashupatinath	3.583 to 83.686	37.499 ± 12.034	1.781 to 106.809	37.451 ± 16.831	4.761 to 119.834	46.406 ± 17.023	59.801 to 219.705	121.358 ± 27.143
Patan Durbar Square	18.963 to 86.327	44.506 ± 10.830	3.552 to 103.943	39.254 ± 17.234	13.552 to 117.552	52.668 ± 14.500	81.636 to 212.822	136.429 ± 20.118
Swayambhunath	12.502 to 76.937	37.044 ± 9.062	2.996 to 115.293	38.051 ± 16.339	4.968 to 108.718	44.254 ± 14.709	56.704 to 195.538	119.350 ± 20.024
World average [1]		18		15		27		60

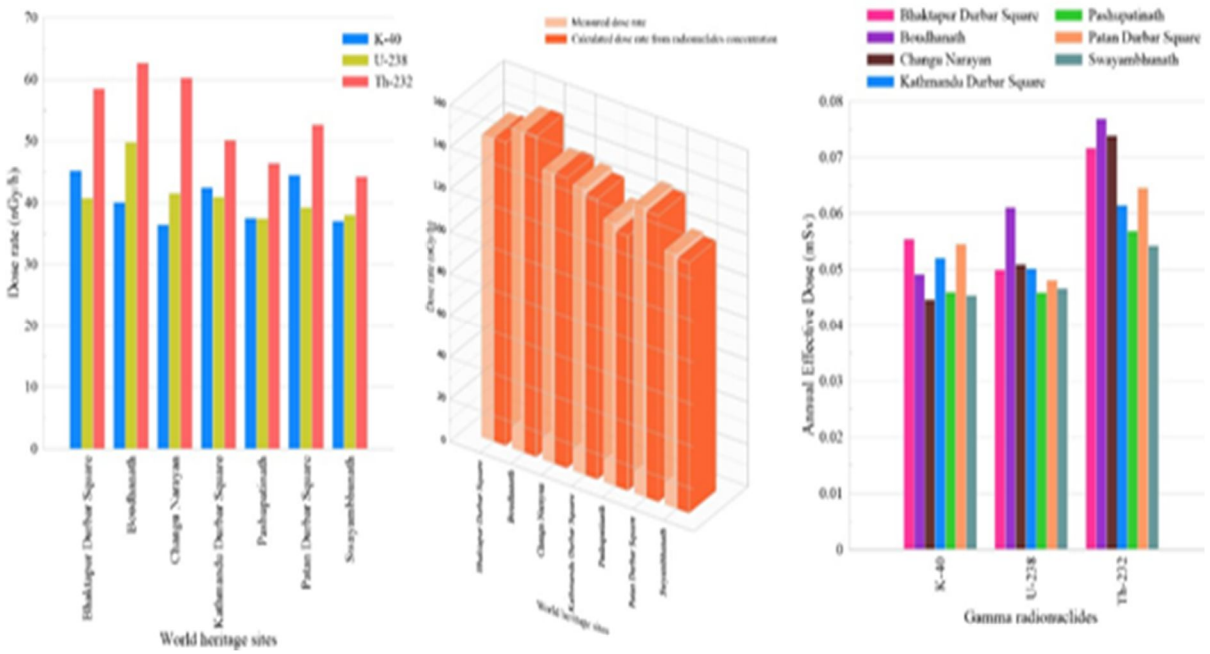

FIG. 1. Dose rates and AED of seven UNESCO World Heritage Sites.

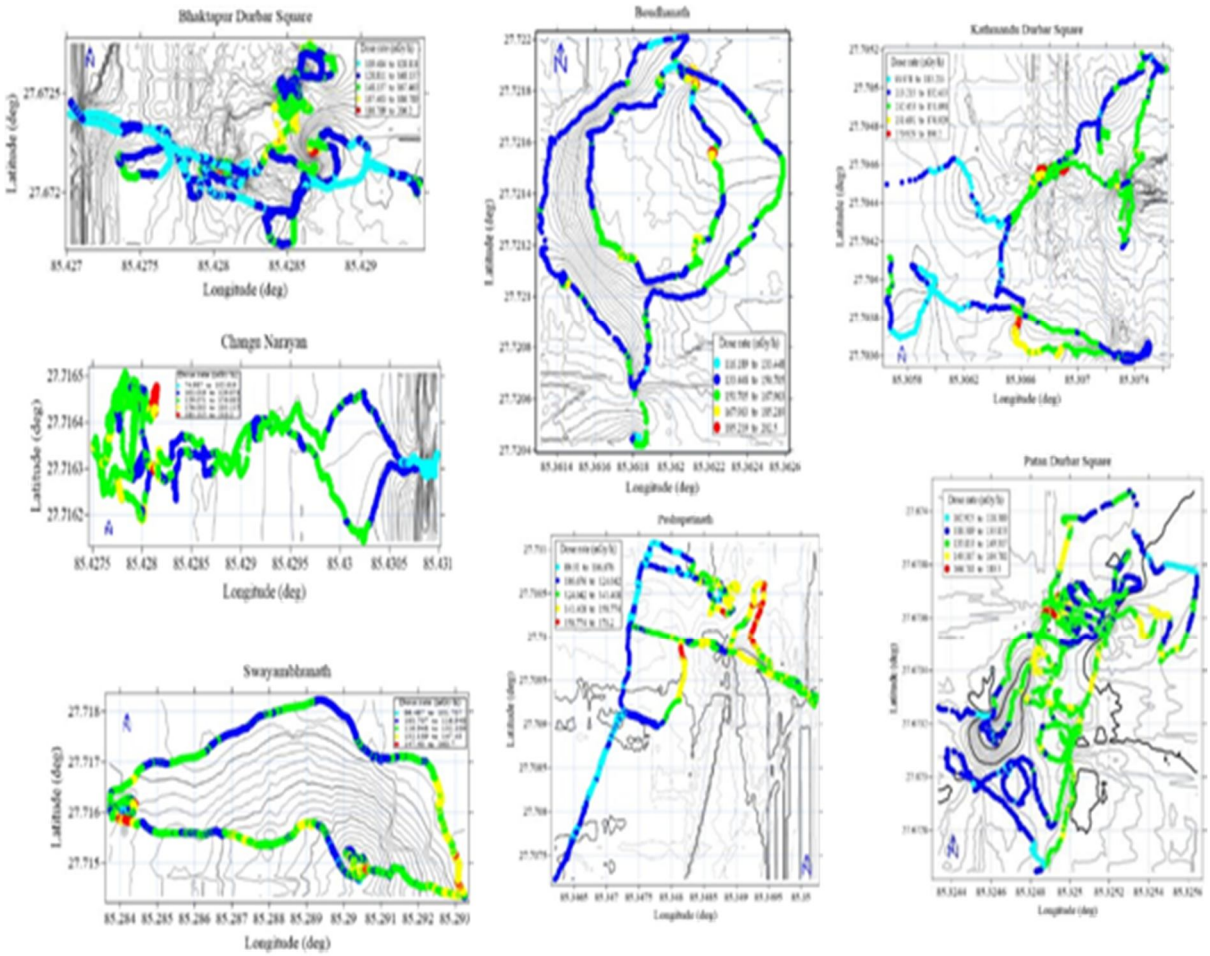

FIG. 2. Measured absorbed dose rates overlaid on topographical maps showing altitude contours.

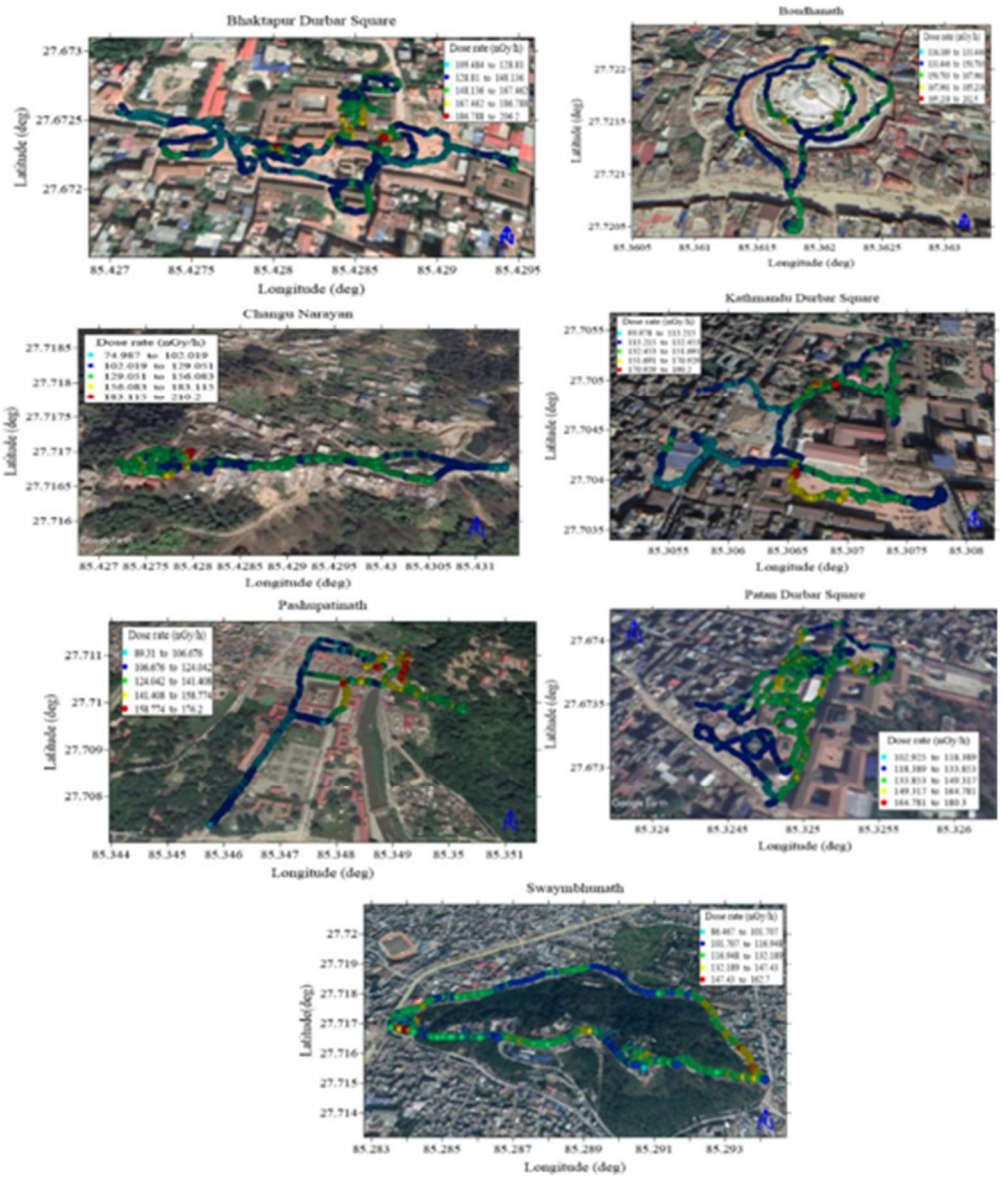

FIG. 3. Measured absorbed dose rates map overlaid on imagery map.

The average outdoor AED from ^{40}K was found from 0.045 to 0.055 mSv (Table 4) which was found higher than the world average external AED value of 0.150 mSv from ^{40}K [15]. Similarly, the average outdoor AED from ^{238}U and ^{232}Th were found in the range 0.045 to 0.061mSv and 0.054 to 0.076 mSv which were also higher than the world average external AED value of 0.100 mSv and 0.160 mSv as reported for ^{238}U and ^{232}Th, respectively [15]. The annual effective dose from ^{40}K was found higher in Bhaktapur Durbar Square and lower in Changu Narayan while AED from ^{238}U and ^{232}Th was found higher in Boudhanath and lower in Pashupatinath (Fig. 1). The AED for each site was estimated from the total measured dose rates yielding a minimum of 0.148 ± 0.013 mSv in Swayambhunath and maximum of 0.18 ± 0.018 mSv in Boudhanath (Table 5). Radiological risk was assessed by calculating ELCR (Table 5). The ELCR value was found in the range of 0.539×10^{-3} ± 0.049×10^{-3} to 0.680 $\times10^{-3}$ $\pm0.067\times10^{-3}$. These figures exceed the world average value of 0.29×10^{-3} [13]. The average ELCR was found 0.95 in Palestine, which is 3.27 times higher than the world average value but the negligible risk of developing cancer has been stated [16]. In most of the study, mortality and ELCR has not been linked with the population of that area.

The statistical analysis was performed at a 0.05 level of significance (Table 6). The histogram of the dose rate showed that the distribution of the data is asymmetric (Fig. 4). The data on the dose rate of UNESCO World Heritage Sites were skewed right with kurtosis.

TABLE 4. Outdoor Annual Effective Dose from gamma radionuclides ^{40}K, ^{238}U and ^{232}Th estimated from the dose rates calculated from mass concentrations

Sites	AED (mSv)					
	^{40}K		^{238}U		^{232}Th	
	Range	Mean	Range	Mean	Range	Mean
Bhaktapur Durbar Square	0.022 to 0.104	0.055 ± 0.012	0.004 to 0.134	0.050 ± 0.021	0.016 to 0.160	0.071 ± 0.020
Boudhanath	0.012 to 0.087	0.049 ± 0.011	0.006 to 0.154	0.061 ± 0.023	0.026 to 0.145	0.076 ± 0.021
Changu Narayan	0.007 to 0.087	0.044 ± 0.011	0.007 to 0.158	0.050 ± 0.023	0.006 to 0.171	0.073 ± 0.024
Kathmandu Durbar Square	0.017 to 0.106	0.052 ± 0.013	0.004 to 0.146	0.050 ± 0.022	0.006 to 0.171	0.061 ± 0.020
Pashupatinath	0.004 to 0.102	0.045 ± 0.014	0.002 to 0.130	0.045 ± 0.020	0.005 to 0.146	0.056 ± 0.020
Patan Durbar Square	0.023 to 0.105	0.054 ± 0.013	0.004 to 0.127	0.048 ± 0.021	0.016 to 0.144	0.064 ± 0.017
Swayambhunath	0.015 to 0.094	0.045 ± 0.011	0.003 to 0.141	0.046 ± 0.020	0.006 to 0.133	0.054 ± 0.018

TABLE 5. Outdoor AED and ELCR calculated from measured dose rates.

Sites	AED		ELCR×10^{-3}	
	Range	Mean	Range	Mean
Bhaktapur Durbar Square	0.134 to 0.252	0.176± 0.019	0.488 to 0.920	0.643±0.070
Boudhanath	0.142 to 0.248	0.186±0.018	0.518 to 0.904	0.680±0.067
Changu Narayan	0.091 to 0.257	0.169±0.025	0.334 to 0.938	0.615±0.092
Kathmandu Durbar Square	0.115 to 0.233	0.166±0.022	0.419 to 0.849	0.607±0.082
Pashupatinath	0.109 to 0.216	0.153±0.023	0.398 to 0.786	0.557±0.085
Patan Durbar Square	0.126 to 0.221	0.169±0.013	0.459 to 0.804	0.616±0.050
Swayambhunath	0.106 to 0.199	0.148±0.013	0.386 to 0.726	0.539±0.049
World average [15]		0.07		0.29

TABLE 6. Statistical analysis of measured dose rates of UNESCO sites.

	Dose rate (n Gy/h)						
	Bhaktapur Durbar Square	Boudhanath	Changu Narayan	Kathmandu Durbar Square	Pashupatinath	Patan Durbar Square	Swayambhunath
Mean	144.023	152.320	137.946	136.013	124.876	138.004	120.907
Median	143.676	149.041	137.494	135.833	122.910	138.540	120.377
First quartile	131.604	142.215	127.692	123.983	108.238	130.774	113.983
Third quartile	154.043	158.565	146.62	145.614	140.584	144.719	127.321
Standard error	0.333	0.435	0.453	0.455	0.327	0.269	0.179
Variance	250.148	227.167	430.166	339.494	363.669	127.250	123.724
Average deviation	12.558	11.472	14.239	14.040	16.727	8.762	8.454
Standard deviation	15.816	15.072	20.740	18.425	19.070	11.280	11.123
Coefficient of variation	0.109	0.098	0.150	0.135	0.152	0.081	0.092
Skew	0.501	0.943	0.445	0.522	0.369	0.074	0.177
Kurtosis	0.49	0.784	2.543	0.465	-0.938	0.466	1.058
Critical K-S stat, alpha=.05	0.029	0.039	0.03	0.033	0.023	0.032	0.022

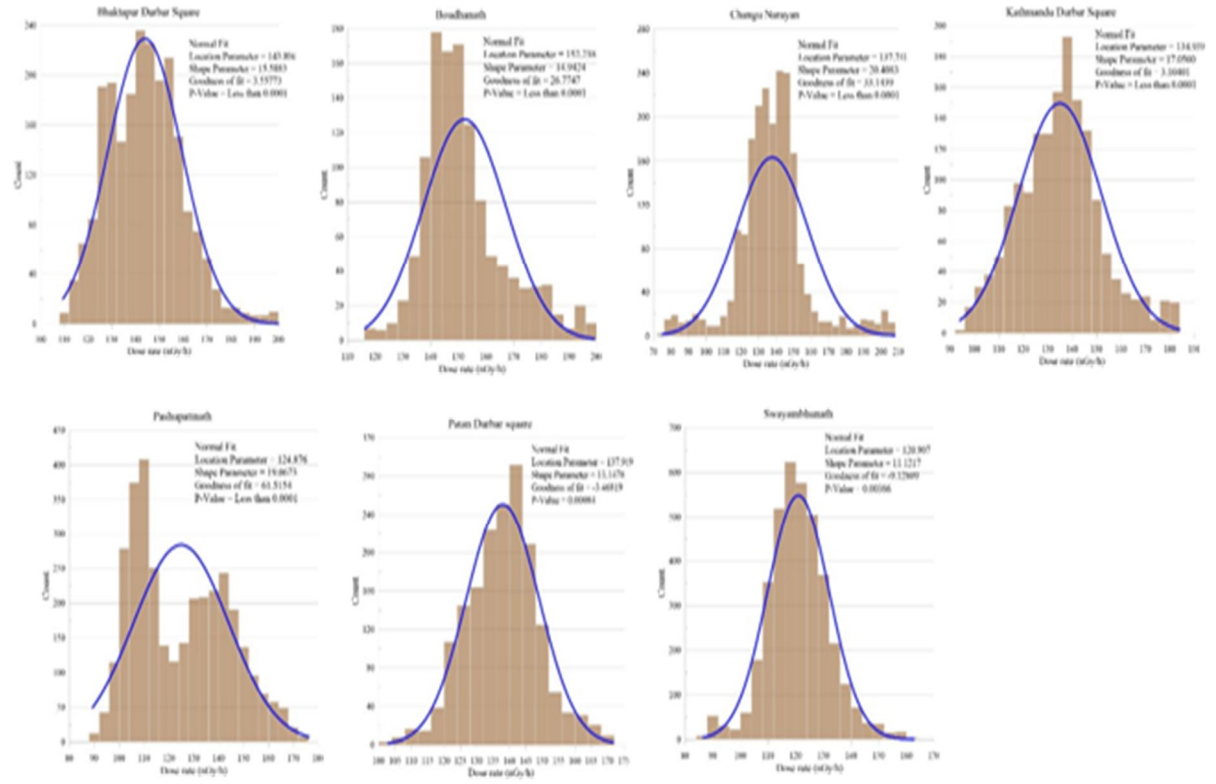

FIG. 4. Dose rates of seven UNESCO World Heritage Sites.

The dose rate of Changu Narayan had high positive kurtosis while the dose rate data of Pashupatinath had negative kurtosis. The goodness of fit and the extremely significant p-value for the dose rate data also showed that the data were not consistent with the normal distribution. The shifted median and the outliers in the box-whisker plot of dose rate and mass concentration of gamma radionuclides ^{40}K, ^{238}U, and ^{232}Th also showed that the data were skewed right (Fig. 5). The box size showed that the dispersion of mass concentration data of ^{40}K was high in Pashupatinath whereas the dispersion of mass concentration data of ^{238}U and ^{232}Th were high in Changu Narayan. In terms of location, the data on the dose rate exhibited a higher level of dispersion in Pashupatinath. At the same time, the data on the calculated dose rate from the mass concentration of gamma radionuclides ^{40}K, ^{238}U, and ^{232}Th were found more dispersed than the data on the measured dose rate. The scatter plot showed a positive and linear correlation between the dose rates and the mass concentrations of gamma radionuclides (Fig. 6). The regression analysis indicated that the dose rate of Bhaktapur Durbar Square depends 64.95%, 79.43%, and 40.3% on mass concentrations of ^{232}Th, ^{40}K, and ^{238}U, respectively. Similarly, the dose rate dependence on mass concentrations of ^{232}Th ^{40}K, and ^{238}U data showed the following numbers: 59.5%, 48.3%, and 47.3% in Boudhanath; 78.62%, 67.9%, and 56.39% in Changu Narayan; 79%, 80.17%, and 43.56% in Pashupatinath; 74.99%, 76.50%, and 58.15% in Kathmandu Durbar Square; 51.14%, 63.34%, and 40.69% in Patan Durbar Square; 68.54%, 60.24%, and 37.73% in Swayambhunath. The contour map of the dose rates showed that the spatial distribution of dose rates is smooth in the area (Fig. 7).

The outdoor AED of the sites was found 2.114 to 2.657 times higher than the world average of 0.07 mSv [1]. The terrestrial radionuclides present in rocks and river sediments at higher altitudes contribute to the high radiation level in the sites of such geological areas. For example, the terrestrial radiation dose was found higher in Indian states bordering Nepal: 885-900 μGy/y in Bihar, 800 μGy/y in Uttar Pradesh, and 877 μGy/y in West Bengal [17]. Likewise, a higher terrestrial radiation dose rate with a mean value of 209±8 nGy/h and a maximum dose rate of 500 nGy/h has been reported in the Kelantan state of Malaysia [18]. Yet another instance of this phenomenon is observed in Madi Hamlet, Yangjiang in Guangdong province of China where the outdoor dose range varies from

0.22±0.003 to 0.36±0.017 μGy/h in [19]. Also, high dose rates were reported in Pakistan and Nigeria [20], [21]. The high content of radionuclides present in the building materials can also contribute to high levels of gamma radiation [22], [23], [24], [25]. Even though the AED value of outdoor terrestrial gamma radiation in the sites was found above the world average value of 0.07 mSv [1], they are still below the dose limit of 1 mSv/y for humans as recommended by ICRP [14]. Consequently, the measured level of radiation in these sites is not considered hazardous to the health of people present in these areas. Moreover, some studies suggest that low radiation exposure is actually beneficial for humans. Thus, low radiation is used for curing infections, aiding rapid wound healing, relieving pain caused by arthritis, and inhibiting the growth and occurrence of tumors [26], [27], [28]. At the same time, exposure to natural background radiation was not found to increase the risk of acute leukemia [29]. On the contrary, there are records of both recovery and adaptation to low-dose radiation [30]. Moreover, life expectancy was found longer in people living in high background radiation areas compared to low background radiation areas [31]. Hence, the radiation doses observed in the sites examined in the present study show no associated health risks for visitors, pilgrims, shopkeepers, and the surrounding areas' inhabitants.

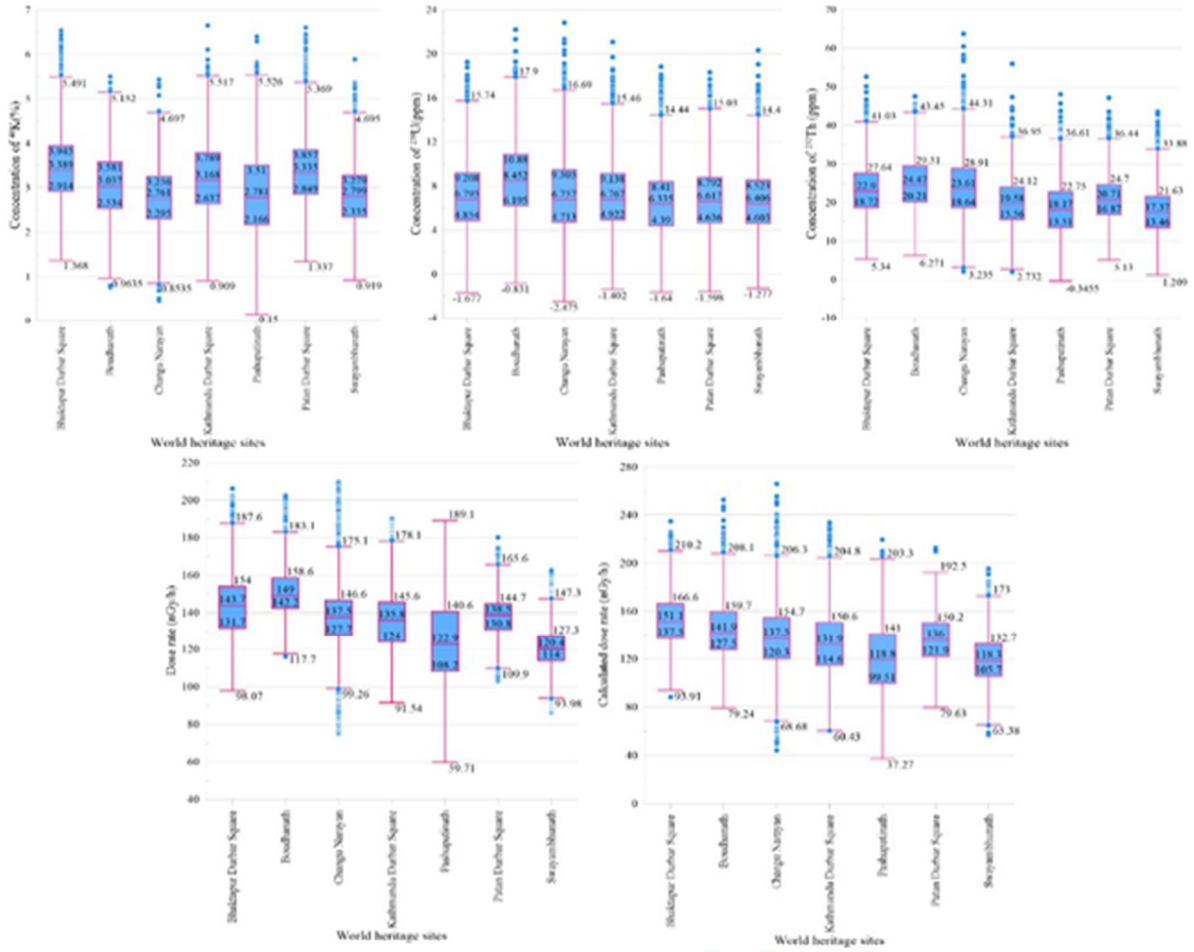

FIG. 5. Mass concentrations of gamma radionuclides ^{40}K, ^{238}U and ^{232}Th and dose rates.


Bhaktapur Durbar Square
RMA Fit
Y = 3.6892 * X + 57.584
Coefficient of determination, R-sq(d) = 0.6405
Correlation coefficient, R = 0.8059
P-Value = Less than 0.0001
Dose rate (mGy/ka)
Concentration of 232Th(ppm)
Bhaktapur Durbar Square
RMA Fit
Y = 26.845 * X + 53.911
Coefficient of determination, R-sq(d) = 0.7593
Correlation coefficient, R = 0.8712
P-Value = Less than 0.0001
Dose rate (mGy/ka)
Concentration of 40K(%)
Bhaktapur Durbar Square
RMA Fit
Y = 9.5473 * X + 75.492
Coefficient of determination, R-sq(d) = 0.4032
Correlation coefficient, R = 0.6350
P-Value = 0.0054
Dose rate (mGy/ka)
Concentration of 238Uppm)
Boudhanath
RMA Fit
Y = 3.1638 * X + 72.822
Coefficient of determination, R-sq(d) = 0.5955
Correlation coefficient, R = 0.7717
P-Value = Less than 0.0001
Dose rate (mGy/ka)
Concentration of 232Th(ppm)
Boudhanath
RMA Fit
Y = 25.072 * X + 63.174
Coefficient of determination, R-sq(d) = 0.4831
Correlation coefficient, R = 0.6951
P-Value = 0.0002
Dose rate (mGy/ka)
Concentration of 40K(%)
Boudhanath
RMA Fit
Y = 8.0540 * X + 81.575
Coefficient of determination, R-sq(d) = 0.4736
Correlation coefficient, R = 0.6882
P-Value = 0.0004
Dose rate (mGy/ka)
Concentration of 238Uppm)
Changu Narayan
RMA Fit
Y = 3.3101 * X + 57.510
Coefficient of determination, R-sq(d) = 0.7562
Correlation coefficient, R = 0.8857
P-Value = Less than 0.0001
Dose rate (mGy/ka)
Concentration of 232Th(ppm)
Changu Narayan
RMA Fit
Y = 38.734 * X + 29.948
Coefficient of determination, R-sq(d) = 0.6790
Correlation coefficient, R = 0.8240
P-Value = Less than 0.0001
Dose rate (mGy/ka)
Concentration of 40K(%)
Changu Narayan
RMA Fit
Y = 10.731 * X + 59.311
Coefficient of determination, R-sq(d) = 0.5639
Correlation coefficient, R = 0.7509
P-Value = Less than 0.0001
Dose rate (mGy/ka)
Concentration of 238Uppm)
Kathmandu Durbar Square
RMA Fit
Y = 4.0501 * X + 54.564
Coefficient of determination, R-sq(d) = 0.7499
Correlation coefficient, R = 0.8660
P-Value = Less than 0.0001
Dose rate (mGy/ka)
Concentration of 232Th (ppm)
Kathmandu Durbar Square
RMA Fit
Y = 28.329 * X + 44.006
Coefficient of determination, R-sq(d) = 0.7650
Correlation coefficient, R = 0.8746
P-Value = Less than 0.0001
Dose rate (mGy/ka)
Concentration of 40K (%)
Kathmandu Durbar Square
RMA Fit
Y = 10.511 * X + 60.266
Coefficient of determination, R-sq(d) = 0.5615
Correlation coefficient, R = 0.7526
P-Value = Less than 0.0001
Dose rate (mGy/ka)
Concentration of 238U (ppm)

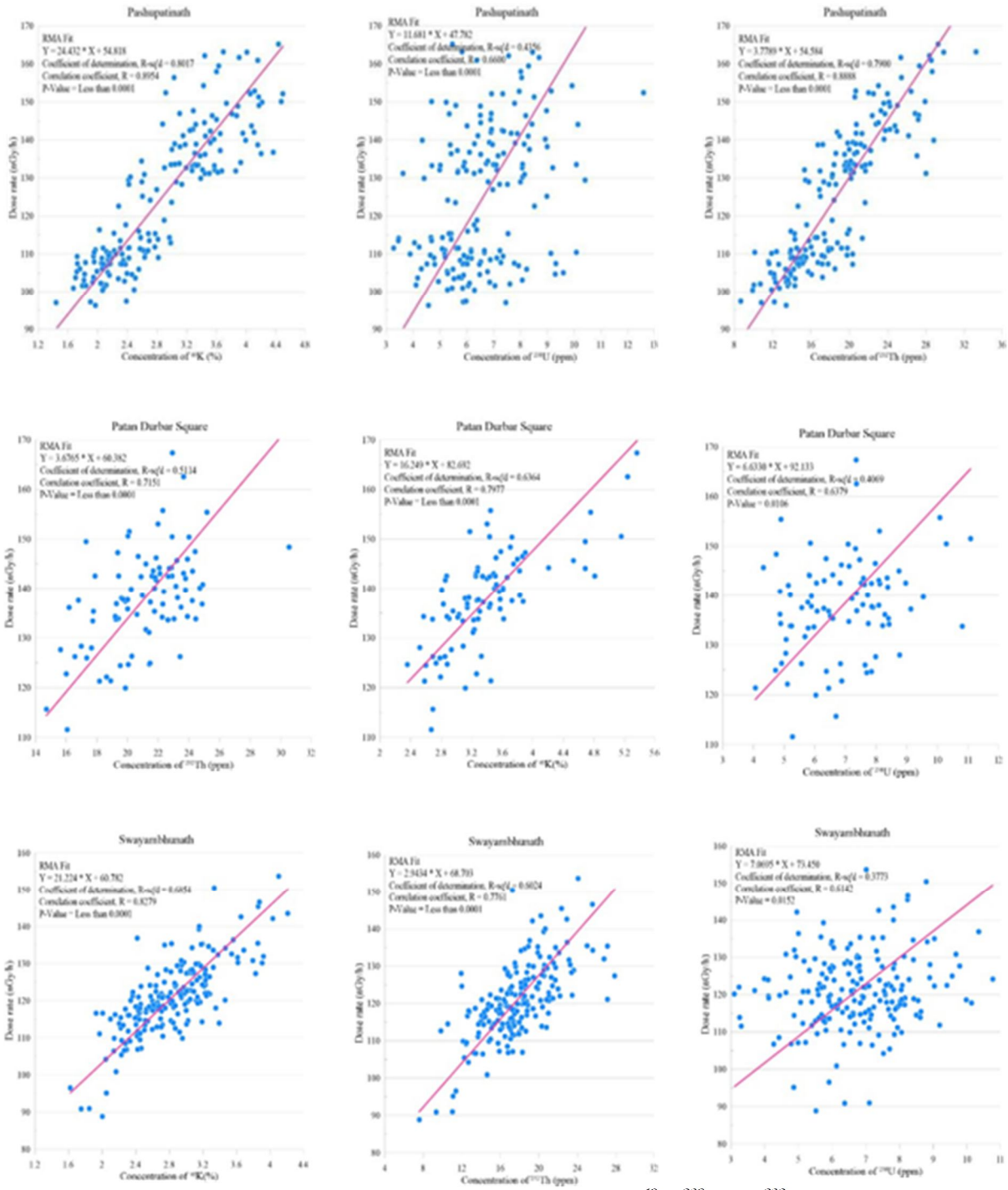

FIG. 6. Dose rates with mass concentrations of gamma radionuclides ^{40}K, ^{238}U and ^{232}Th of seven UNESCO World Heritage Sites.

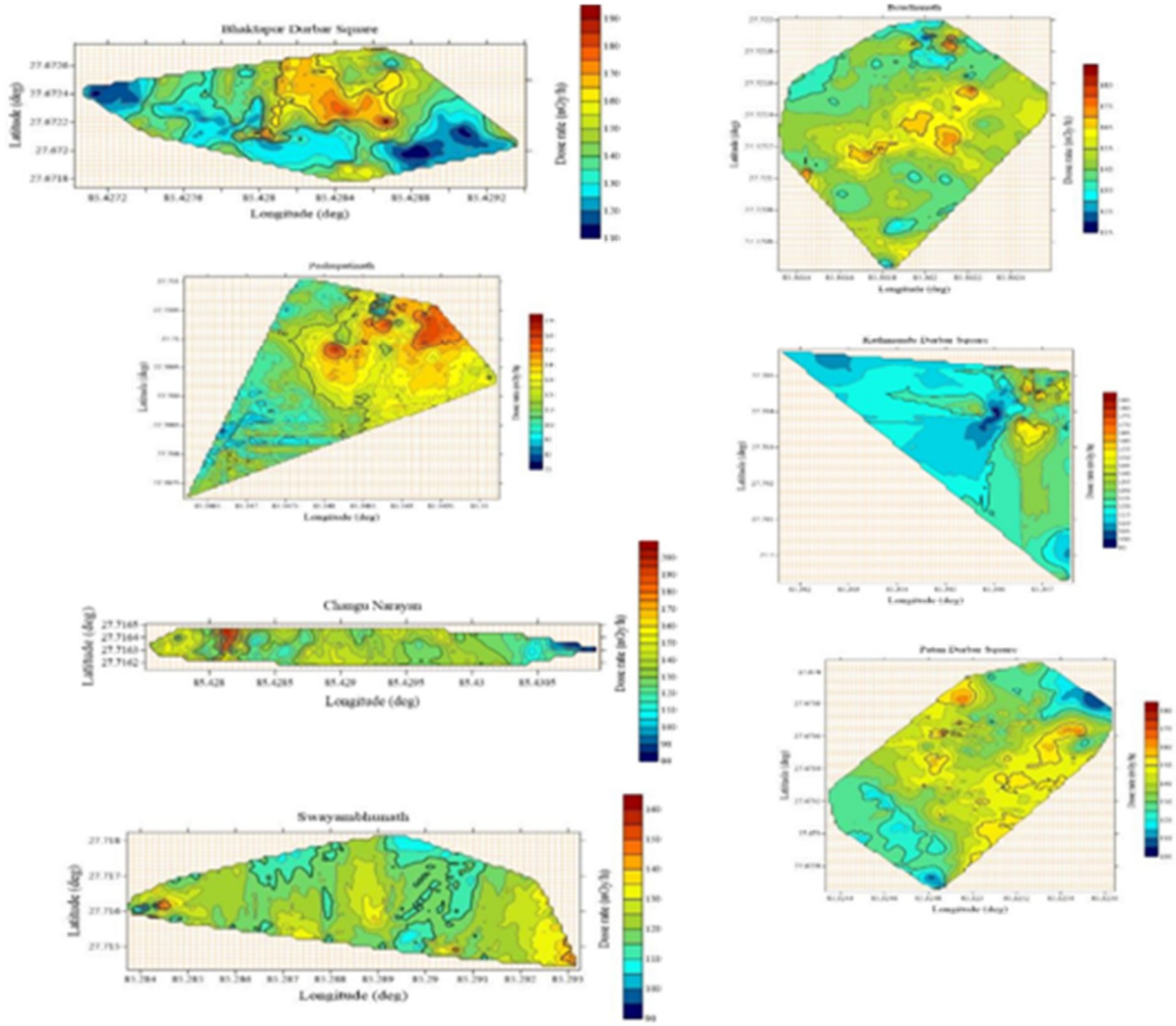

FIG. 7. Dose rates contour map of seven UNESCO World Heritage Sites.

Conclusion

The outdoor absorbed dose rates in the air from gamma radiation and the mass concentrations of radioelement ^{40}K, ^{238}U, and ^{232}Th present in building materials and the Earth's surface have been measured in the seven UNESCO Cultural Heritage Sites located in the Kathmandu Valley of Nepal using the in-situ gamma-ray spectrometric method. The absorbed dose rates in the air and mass concentrations of radioelement were found higher than the world average value as reported in UNSCEAR. The dose rates for the particular radioelements were also calculated from their mass concentration and were found nearly equal to the measured dose rates. The statistical analysis showed that the data is skewed right and the dose rates have a positive correlation with the gamma radionuclides. The associated health risk ELCR was calculated using AED for the visitors, pilgrims, shopkeepers, and inhabitants. The outdoor AED calculated was found higher than the world average outdoor AED from terrestrial radiation but is below the dose limit for the public as recommended by ICRP. Thus, the sites do not pose any risks to human health. The obtained results are expected to form baseline data. Further epidemiological studies may be needed to suggest possible health hazards for the public.

Acknowledgements

We acknowledge the support from the IAEA (through TC project NEP0002), the Ministry of Education, Science and Technology, the Government of Nepal (for coordination with IAEA), and the University Grants Commission, Nepal (for Ph.D. fellowship to Anita Mishra, award number Ph.D.- 74/75-S&T-15).

References

[1] United Nations Scientific Committee on the Effects of Atomic Radiation, "Sources and Effects of Ionizing Radiation", Annex B, UNSCEAR Report. 1, (2000).

[2] International Atomic Energy Agency, "Guidelines for Radioelement Mapping Using Gamma Ray Spectrometry Data", report IAEA-TECDOC-1363, (2003).

[3] Tzortzis, M. and Tsertos, H., J. Environ. Radioact, 77 (3) (2004) 325.

[4] Santos Junior, J.A.D. *et al.*, Braz. Arch. Biol., 48 (2005) 221.

[5] Lee, E.M., Menezes, G. and Finch, E.C., Health Phys., 86 (4) (2004) 378.

[6] Papastefanou, C., Stoulos, C.S. and Manolopoulou, M., J. Radioanal. Nucl., 266 (3) (2005) 367.

[7] International Atomic Energy Agency. "The Use of Gamma Ray Data to Define the Natural Radiation Environment", technical report IAEA-TECDOC-566, (1990).

[8] Hosoda M. *et al.* PLoS One, 10 (4) (2015) e0124433.

[9] Li, B. *et al.*, J. Environ. Radioact., 151 (2016) 304.

[10] Inoue, K., Arai, M., Fujisawa, M., Saito, K. and Fukushi, M., PLoS One, 12 (1) (2017) e0171100.

[11] Lee, S.K., Wagiran, H., Ramli, A.T., Apriantoro, N.H. and Wood, A.K., J. Environ. Radioact., 100 (5) (2009) 368.

[12] Kaniu, M.I., Angeyo, H.K., Darby, I.G. and Muia, L.M., J. Environ. Radioact., 188 (2018) 47.

[13] Taskin, H. *et al.*, J. Environ. Radioact., 100 (1) (2009) 49.

[14] International Commission of Radiological Protection, "The 2007 Recommendations of the International Commission on Radiological Protection", ICRP publication 103. Ann ICRP. 37 (2007).

[15] United Nations Scientific Committee on the Effects of Atomic Radiation, "Exposures from Natural Radiation Sources", UNSCEAR Report (1988).

[16] Thabayneh, K., Open J. Soil Sci., 2 (1) (2012) 7.

[17] Sankaran, A.V., Jayaswal, B., Nambi, K.S.V. and Sunta. C.M., "U, Th and K Distributions Inferred from Regional Geology and the Terrestrial Radiation Profiles in India", Bhabha Atomic Research centre, Report (1986).

[18] Garba, N.N., Ramli, A.T., Saleh, M.A., Sanusi, M.S. and Gabdo, H.T., J. Radioanal. Nucl., 302 (1) (2014) 201.

[19] Morishima H. *et al.*, J. Radiat. Res., 41 SUPPL (2000) S9.

[20] Khan, I.U., Qin, Z., Xie, T., Bin, Z., Li, H., Sun, W. and Lewis E., Int. J. Radiat. Res., 18 (2) (2020) 243.

[21] Olagbaju, P.O., Okeyode, I.C., Alatise, O.O. and Bada, B.S., Int. J. Radiat. Res., 19 (3) (2021) 591.

[22] Raghu, Y., Ravisankar, R., Chandrasekaran, A., Vijayagopal, P. and Venkatraman, B., J. Taibah Univ. Sci., 11 (4) (2017) 523.

[23] Kuzmanovi, P., Todorovi´c, N., Petrovi´c, L.P., Mrda, D., Forkapi´c, S., Nikolov, J. and Kne˘zevi´c, J., J. Radioanal. Nucl. Chem., 324 (3) (2020) 1077.

[24] Senthil Kumar, C.K, Chandrasekaran, A., Harikrishnan, N. and Ravisankar, R., J. Environ. Anal. Chem., 102 (17) (2020) 5432.

[25] Tuo, F., Peng, X., Zhou, Q. and Zhang, J., Radiat. Prot. Dosim, 188 (3) (2020) 316.

[26] Cuttler, J.M., Dose-Response, 11 (4) (2013).

[27] Mishra, K.P., Ahmed, M. and Hill, R.P., Int. J. Radiat. Biol., 84 (5) (2008) 441.

[28] Pandey, B.N., Sarma, H.D., Shukla, D. and Mishra, K.P., J. Radiat. Res., 2, (1-2) (2006) 111.

[29] Berlivet, J. *et al,* J. Environ. Radioact., 233, (2021) 106613.

[30] Nishad, S., Chauhan, P.K., Sowdhamini, R. and Ghosh, A., Sci. Rep., 11 (1) (2021) 1.

[31] David, E., Wolfson, M. and Fraifeld, V.E., Biogerontology, 22 (2), (2021) 189.

[32] United Nations Scientific Committee on the Effects of Atomic Radiation, "Sources and Effects of Ionizing Radiation", UNSCEAR Report. (2008).